



# Fluid Flow and Heat Transfer in a Heat Exchanger Channel with Short-Length Twisted Tape Turbulator Inserts

Suvanjan Bhattacharyya<sup>1,2</sup>

Received: 27 February 2018 / Accepted: 22 August 2018 / Published online: 4 September 2018  
© Shiraz University 2018

## Abstract

The thermohydraulic characteristics of turbulent flow of air ( $Pr$  0.7) through circular tube with short-length and full-length twisted-tape turbulators inserts have been studied experimentally. Also, heat transfer performance for different values of the twist ratio, tape thickness ratio and diameter ratio are investigated for Reynolds numbers within the range 6000–20,000. The full-length twisted tape enhances heat transfer more than those of short-length twisted tapes. Heat transfer and pressure drop tests were carried out in brass channels. The channel with twisted tape inserts specifies that the use of tapes augments heat transfer mostly, which is complemented by a greater friction penalty. The thermohydraulic performance of the problem under study has been assessed. It is observed that by using full-length twisted tape at constant pumping power, up to 27% heat duty rises in comparison with short-length twisted tape. Similarly, by using full-length twisted tape at heat duty, up to 33% pumping power increases in comparison with short-length twisted tape.

**Keywords** Turbulent flow · Twisted tape · Swirl flow · Heat transfer · Heat exchanger · Forced convection

## List of symbols

$A$	Heat transfer area [ $\pi DL$ ( $m^2$ )]
$A_0$	Plain duct flow cross-sectional area ( $m^2$ )
$C_p$	Constant pressure specific heat (J/kg K)
$D$	Internal diameter of the plain channel (m)
$D_h$	Hydraulic diameter of the test duct = $4A_0/P$ (m)
$f$	Fully developed Fanning friction factor (dimensionless)
FLTT	Full-length twisted-tape
FLHT	Full-length helical tape
$g$	Gravitational acceleration ( $m/s^2$ )
$Gr$	Grashof number = $g\beta\rho^2D_h^3\Delta T_w/\mu^2$ (dimensionless)
$H$	Pitch for 180° rotation of twisted tape (m)
$h_z$	Axially local heat transfer coefficient [ $W/(m^2 K)$ ]
$k$	Fluid thermal conductivity [ $W/(mK)$ ]
$L$	Length of twisted-tape (m)

$m$	Mass flow rate (kg/min)
$Nu_m$	Axially averaged Nusselt number = $\frac{1}{L} \int_0^L \frac{h_z D_h dz}{k}$ (dimensionless)
$\Delta P_z$	Pressure drop (mm)
$P$	Wetted perimeter in the particular cross section of the duct (m)
$Pr$	Fluid Prandtl number = $\mu C_p/k$ (dimensionless)
$Ra$	Rayleigh number = $Gr \cdot Pr$
$Re$	Reynolds number based on plain channel diameter (dimensionless)
$T$	Temperature (K)
SLTT	Short-length twisted tape
$\Delta T_w$	Wall to fluid bulk temperature difference (K)
$X$	$Pr^n$ , the value of $n$ depends on the exponent of $Pr$ in the correlation
$Y$	$\left(\frac{\mu_b}{\mu_w}\right)^{-0.14} \times \frac{1}{5.172}$
$y$	Twist ratio (dimensionless)

✉ Suvanjan Bhattacharyya  
suvanjan@mckvie.edu.in; u18394737@tuks.co.za

<sup>1</sup> Department of Mechanical Engineering, MCKV Institute of Engineering, 243 G.T. Road (N), Liluah, Howrah, West Bengal 711204, India

<sup>2</sup> Present Address: Department of Mechanical and Aeronautical Engineering, University of Pretoria, Pretoria 0002, South Africa

## Greek symbols

$\beta$	Coefficient of isobaric thermal expansion ( $K^{-1}$ )
$\delta$	Tape thickness ratio [ $t/D$ (m)]
$\mu$	Fluid dynamic viscosity (kg/ms)
$\rho$	Density of the fluid ( $kg/m^3$ )

## Subscripts

$a_x$	At axial flow condition
$b$	At bulk fluid temperature
$m$	Axially averaged
$sw$	At swirl flow condition
$w$	At duct wall temperature, with
$z$	Local value

## 1 Introduction

Heat exchanger is an equipment facilitating heat transfer (HT) involving two or more fluids. In numerous industries, likely as chemical dispensations, refrigerating systems, air handling units, thermal power plants, air conditioning apparatus, and radiators for space shuttles in addition to automobiles, etc., heat exchanger (HE) is extensively utilized. To increase the performances of heat exchangers, heat transfer enhancement (THE) techniques have been developed. A method for heat transfer enhancement is the insertion of structures into the flow path that favorably alter the flow pattern (Tiwari and Saha 2015; Ghajar et al. 2010; Roy and Saha 2015; Meyer and Abolarin 2018; Saha 2010; Meyer and Olivier 2011; Saha 2011; Rahimi and Soran 2017; Sabet et al. 2017; Bhattacharyya et al. 2018). One of the practical means to this purpose is introducing swirl in a pipe flow by the insertion of a twisted tape (TT) as shown in Fig. 1. This is investigated in the present study.

TT swirl generators are generally engaged for manufacturing compact heat exchangers and increasing the thermal enhancement performance (TEP) of the existing HE due to their low cost and ease of installation. Swirl generators assist in moving fluid from channel core to near wall region and vice versa. Earlier studies have shown that heat transfer enhancement with different working fluids is strongly dependent on different swirl generators geometric factors (Balachandar et al. 2018; Mohammadiun et al. 2017; Sheikholeslami and Ganji 2016a, b; Sheikholeslami et al. 2018; Sheikholeslami and Shehzad 2018; Sheikholeslami 2018a, b; Sheikholeslami and Rokni 2018; Sheikholeslami and Seyednezhad 2018).

In many heat exchanger relevancies, transitional flow conditions may prevail, the modeling of which is more demanding compared to fully turbulent flow, and still not exhaustively explored. In the present study, enrichment of heat transfer in a pipe flow by a twisted tape is experimentally investigated, within a range of Reynolds numbers between 6000 and 20,000.

Early investigations on the channel with twisted tape configurations were performed by Manglik and Bergles (1994) and Al-Fahed and Chakroun (1996). Suresh et al. (2004) studied the theory of the thermohydraulic affectivity of twisted-tape inserts within a bulky hydraulic diameter

annulus. Bhattacharyya and Saha (2012), Bhattacharyya et al. (2013) and Saha et al. (2012) noted down that the center-clearing twisted tapes in amalgamation with rib roughness execute extensively better than the standalone enhancement technique acting single-handedly for laminar flow throughout a duct involving circular geometric cross section up to a convincing range of twisted-tape center-clearance. Sivashanmugam and Suresh (2006, 2007a, b, c) investigated experimentally on the characteristics of the heat transfer and friction factor of the laminar and turbulent flows throughout a circular tube fitted with full-length helical screw tapes involving different twist ratios, including the increasing and decreasing order of twist ratio sets. Eiamsa-ard and Promvong (2005) reported enrichment of heat transfer in a channel involving helical tape swirl generator having regular-spacing with the variation of Reynolds number ranging between 2300 and 8800 utilizing water as working fluid, and accomplished that the full-length helical tape with rod provides the highest rate of heat transfer of about 10% improvement than that of without rod.

The justified adjustment between the enhanced HT and minimum friction penalty can be attained by using twisted tape swirl generators with proper length ratio, tape thickness ratio, twist ratios, etc. So, in this paper, the results of experimental study of the effect of twisted tapes with different diameter, thickness and twist ratios have been presented and discussed. Heat transfer, pressure drop characteristics and performance have been presented. One of the chief objectives of this paper is to report on the combined effect of the thickness, twist and diameter ratios.

## 2 Experimental Setup and Procedure

The experimental setup is shown in Fig. 2. The test section consists of a circular channel with 22 mm inside diameter and a length of 2.0 m. The atmospheric air with a temperature of about 300 K was sucked in by a 7.0-kW blower. A U-tube manometer is employed to determine the pressure drop across the test section. Also, a rotameter is used to measure the flow rate of the working fluid. Using an adjustable valve, the mass flow rate of the air was varied.

Test section for the current study of heat transfer was heated using an electrical nichrome heater. Nichrome wire heater consists of porcelain bead insulation over it. There exists no direct contact between that heater wire and the channel wall. Insulation of fiber glass tape was provided on the channel wall, and then, it was wrapped by the porcelain-bead-insulated nichrome wire. The heat transfer test section was insulated using asbestos rope and glass wool on the heater wire. Finally, the test section was covered with jute bag.

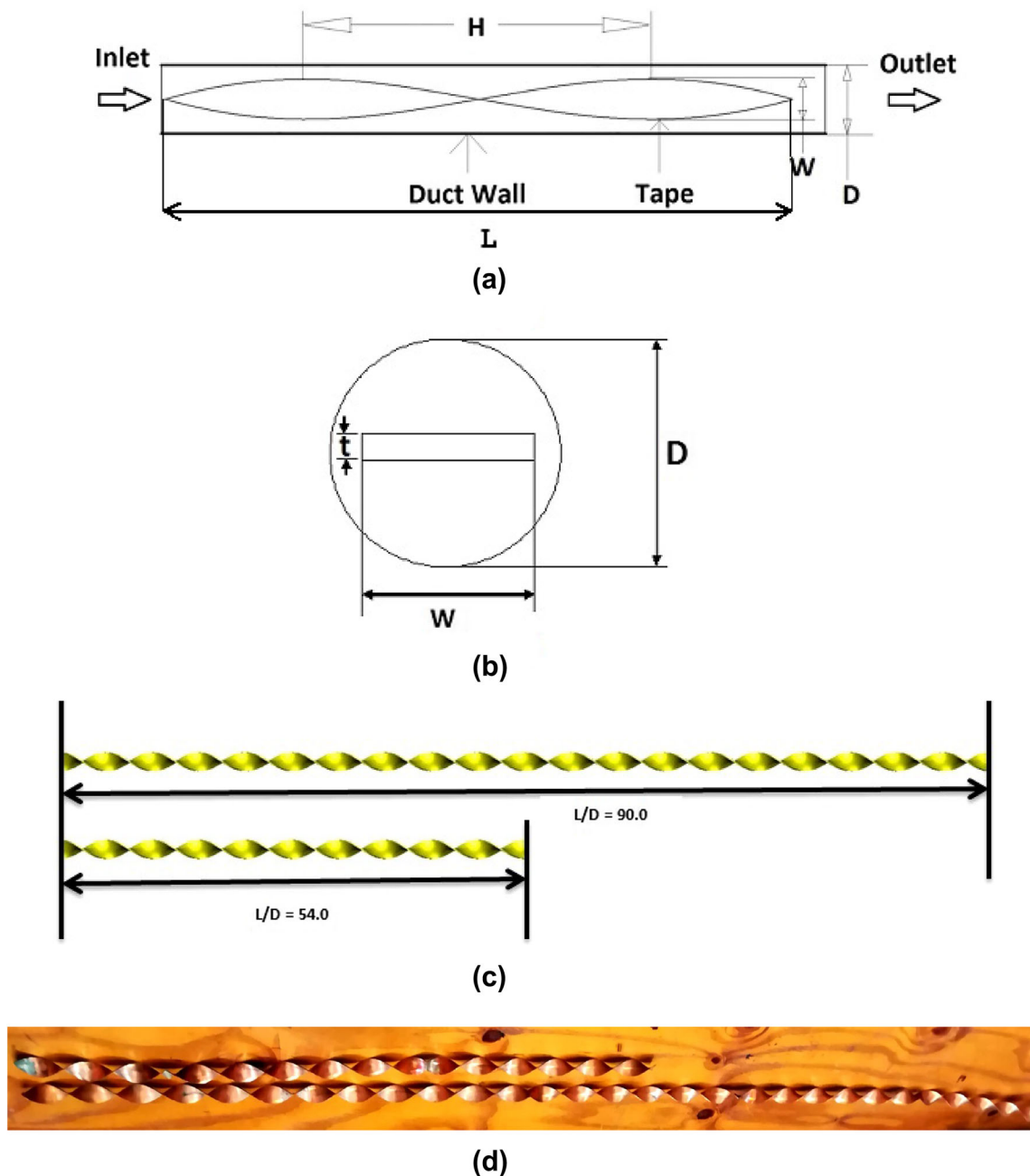


**Fig. 1** **a** Full-length twisted tape, **b** sketch of diameter and tape thickness ratio configuration, **c** sketch of FLTT and SLTT and **d** photographic view of FLTT and SLTT

A selector switch box is used to determine the temperature of the inlet and outlet sections of the test section and also to measure the channel wall temperatures of the test channel. The temperatures of inner and outer walls of the test channel were recorded at seven axial locations, each station having four thermocouples along the channel periphery. This was done with the help of copper–constantan thermocouples and a digital multi-meter. The high thermal conductivity of the channel wall out of brass ( $k = 125 \text{ W/mK}$ ) was facilitated to achieve a quite uniform

inner wall temperature with variations that remain below  $\pm 4\%$  around a mean value of about 340 K. Thus, in the modeling, the assumption of an isothermal condition for the channel wall is found to be reasonable. The measurements of the temperature at peripheral outside wall, at the two locations in an axial station, showed a maximum variation of about 4% at all Reynolds numbers. This variation in the peripheral wall temperature is expected to be principally due to buoyancy and secondary flows.

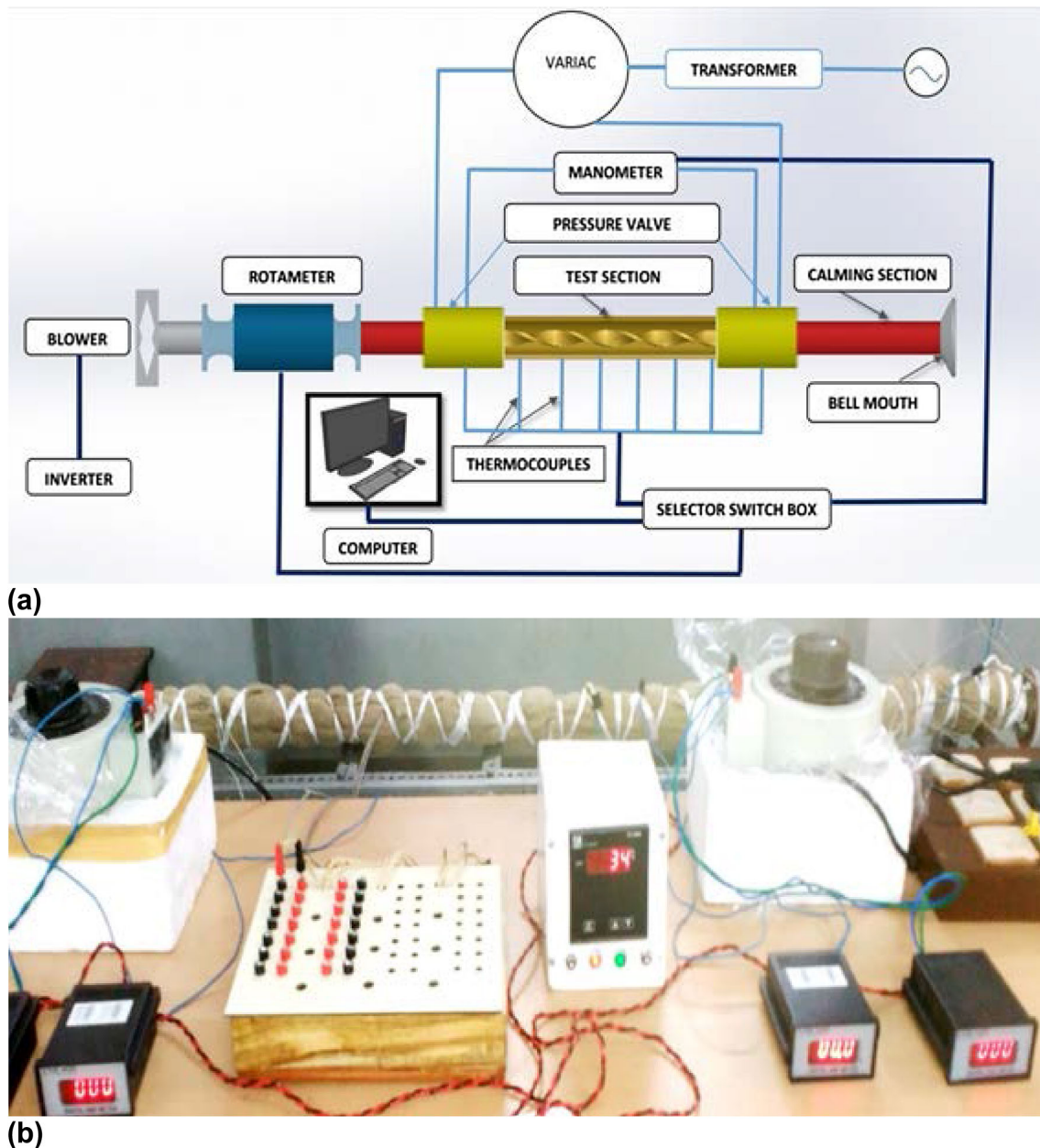


**Fig. 2** **a** Schematic diagram of experimental setup and **b** photographic view

Uncertainties analyses of the major experimental variables are given in Table 1. The uncertainty in Reynolds number, friction factor and Nusselt number was estimated as  $\pm 3.9\%$ ,  $\pm 6.2\%$  and  $\pm 7.1\%$ , respectively, following the procedure of Bhattacharyya et al. (2013).

### 3 Data Reduction

The problem consists of a channel of diameter  $D$  and a twisted tape of thickness ( $\delta = t/D = 0.0417$  and  $0.0458$ ). The length ratio of the twisted tape is about ( $L/D = 90.0$

and  $54.0$ ), where  $L/D = 90.0$  is the full-length twisted tape (FLTT) and  $L/D = 54.0$  is the short-length twisted tape (SLTT). Diameter ratios are considered, namely  $d = W/D = 0.83, 0.75, 0.66$ . The ‘twist ratio’ is defined as  $y = H/D = 15.0$  and  $45.0$  (Fig. 1).

The bulk fluid temperature ( $T_b$ ) is calculated as the arithmetic average of fluid and inlet ( $T_i$ ) outlet ( $T_o$ ) temperatures. The wall heat flux is deduced ( $q_w$ ) from the difference in the energy flow rates of the inflowing and outflowing fluids, with the respective temperatures of  $T_i$  and  $T_o$ .

Heat transferred to the air,  $Q$  can be written by

**Table 1** Experimental uncertainty of major parameters

Name of variables	Errors (%)
Flow velocity ( $v$ )	0.18
Voltage on the heater ( $V$ )	0.15
Electrical resistance ( $R$ )	0.33
Heat transfer coefficient ( $h$ )	1.19
Current on the heater ( $I$ )	0.23
Ambient temperature ( $T_a$ )	0.1
Electrical power on the heater ( $P$ )	0.17
Average temperature ( $T$ )	0.6

$$Q = m_a C_{p,a} (T_o - T_i) \tag{1}$$

where  $m_a$  is the mass flow rate of air,  $C_{p,a}$  is the specific heat of air, and  $T_i$  and  $T_o$  are the inlet and outlet air temperatures, respectively.

In the experiments, the heat equilibrium test showed that the heat absorbed by the air ( $Q$ ) was within 2–4% lower

than the heat supplied by electrical winding; this was due to the heat leakage from the duct wall.

The heat flux rate was calculated by

$$q_w = \frac{Q}{A} \tag{2}$$

where  $A$  is the internal surface area of the channel.

The bulk fluid temperature was obtained by

$$T_b = \frac{T_o + T_i}{2} \tag{3}$$

All the fluid properties were calculated at the average of the inlet and outlet bulk temperatures,  $T_b$ .

The average wall temperature was calculated from

$$T_{wall,Avg} = \sum \frac{T_{wall}}{7} \tag{4}$$

where  $T_{wall}$  is the wall temperature of the channel. The average wall temperature was calculated from seven points of wall temperatures lined between the inlet and the outlet of the test section.

The average heat transfer coefficient was obtained from

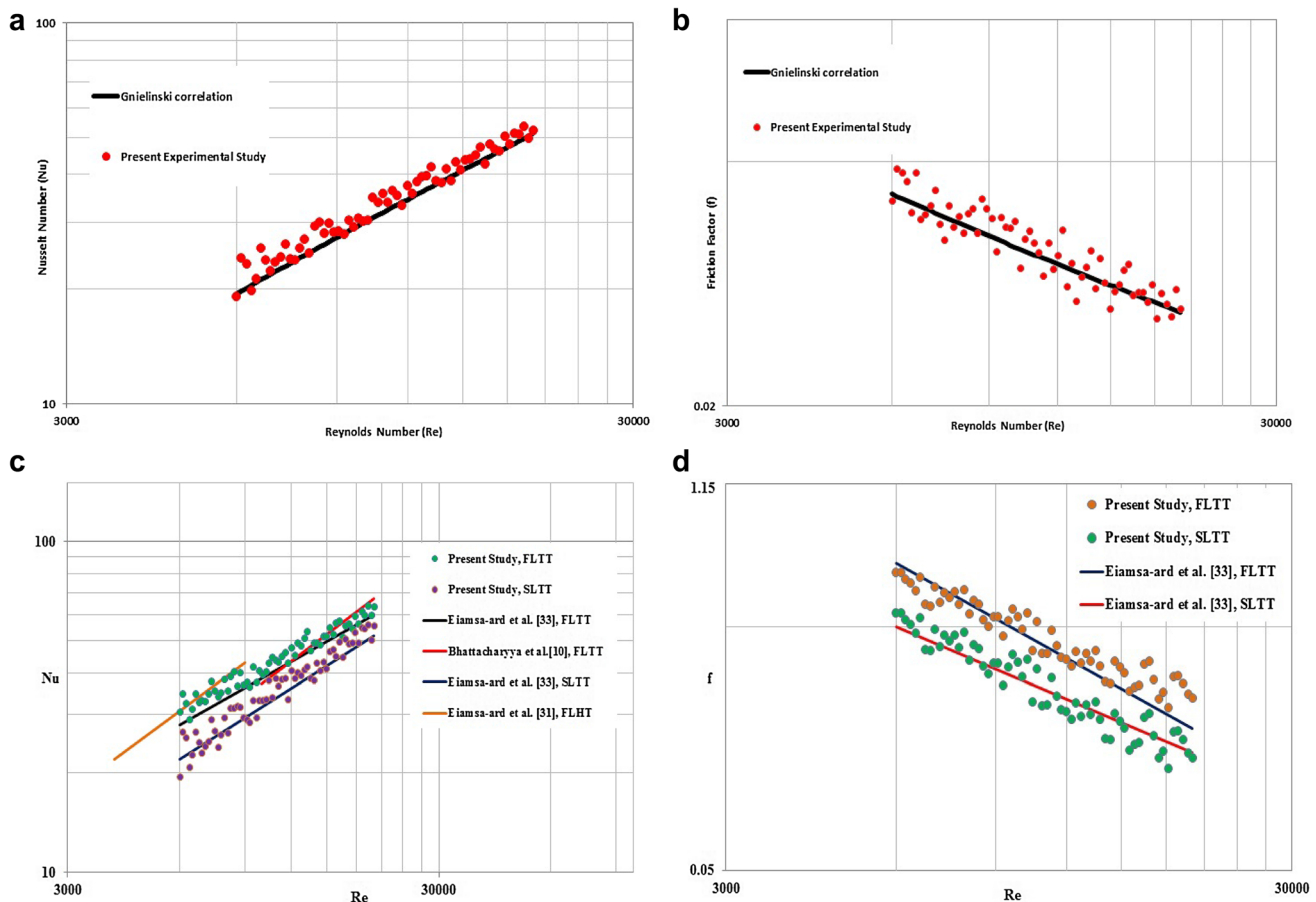
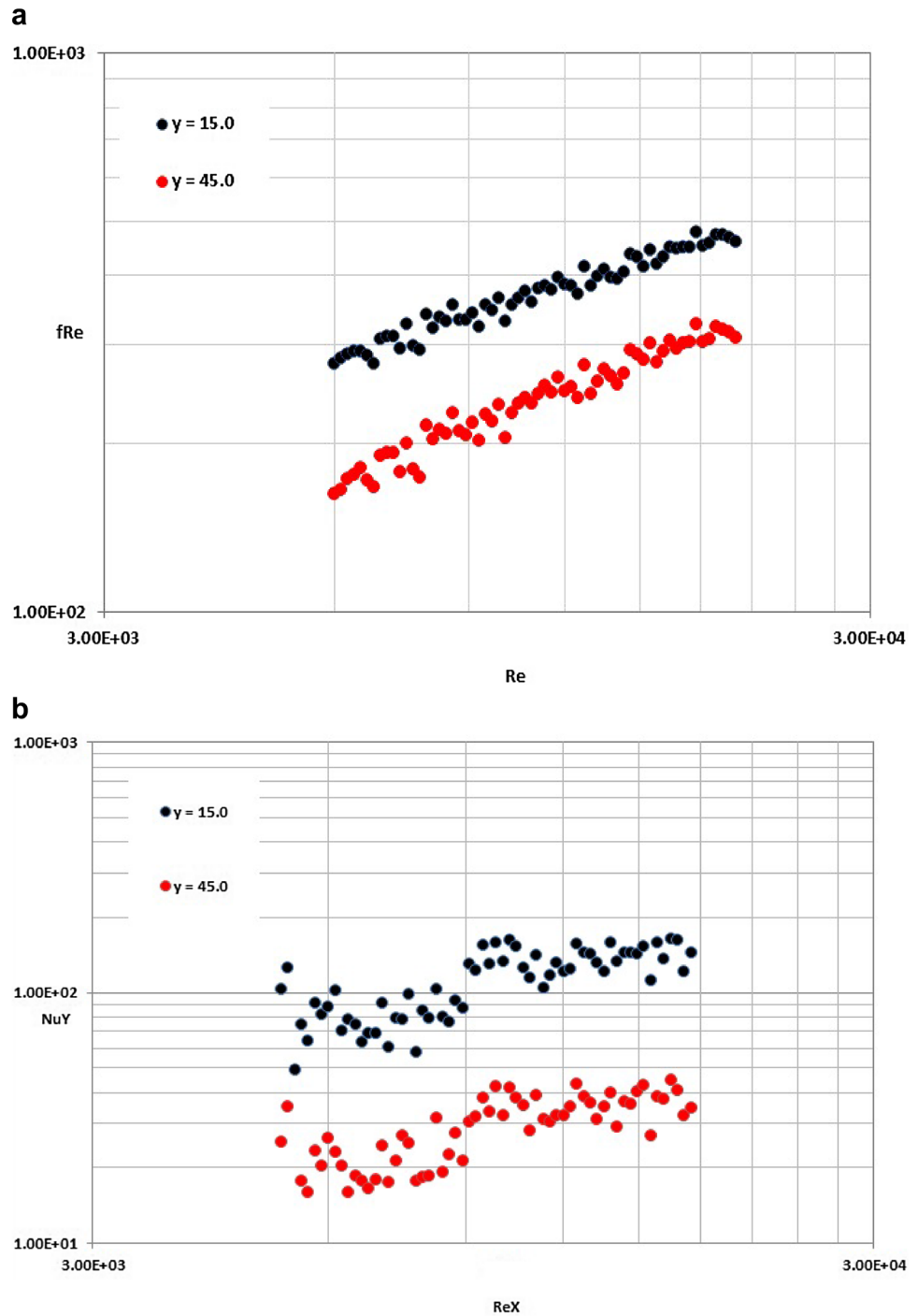


**Fig. 3** **a** Verification of Nusselt number of plain channel, **b** verification of friction factor of plain channel, **c** comparison with the literature of forced convection Nusselt numbers for different swirl

generators and **d** comparison with the literature of forced convection friction factor for different swirl generators

**Fig. 4 a** Effect of twist ratio on friction factor, full-length twisted tape: at constant tape thickness ratio  $\delta = 0.0458$  and diameter ratio  $d = 0.83$  and **b** effect of twist ratio on Nu, full-length twisted tape: at constant tape thickness ratio  $\delta = 0.0458$  and diameter ratio  $d = 0.83$



$$h = \frac{q}{T_{wall,Avg} - T_b} \tag{5}$$

The Nusselt number was calculated according to

$$Nu = \frac{hD_i}{K} \tag{6}$$

where  $k$  is the thermal conductivity of air.

The Reynolds number based on the channel hydraulic diameter is given by

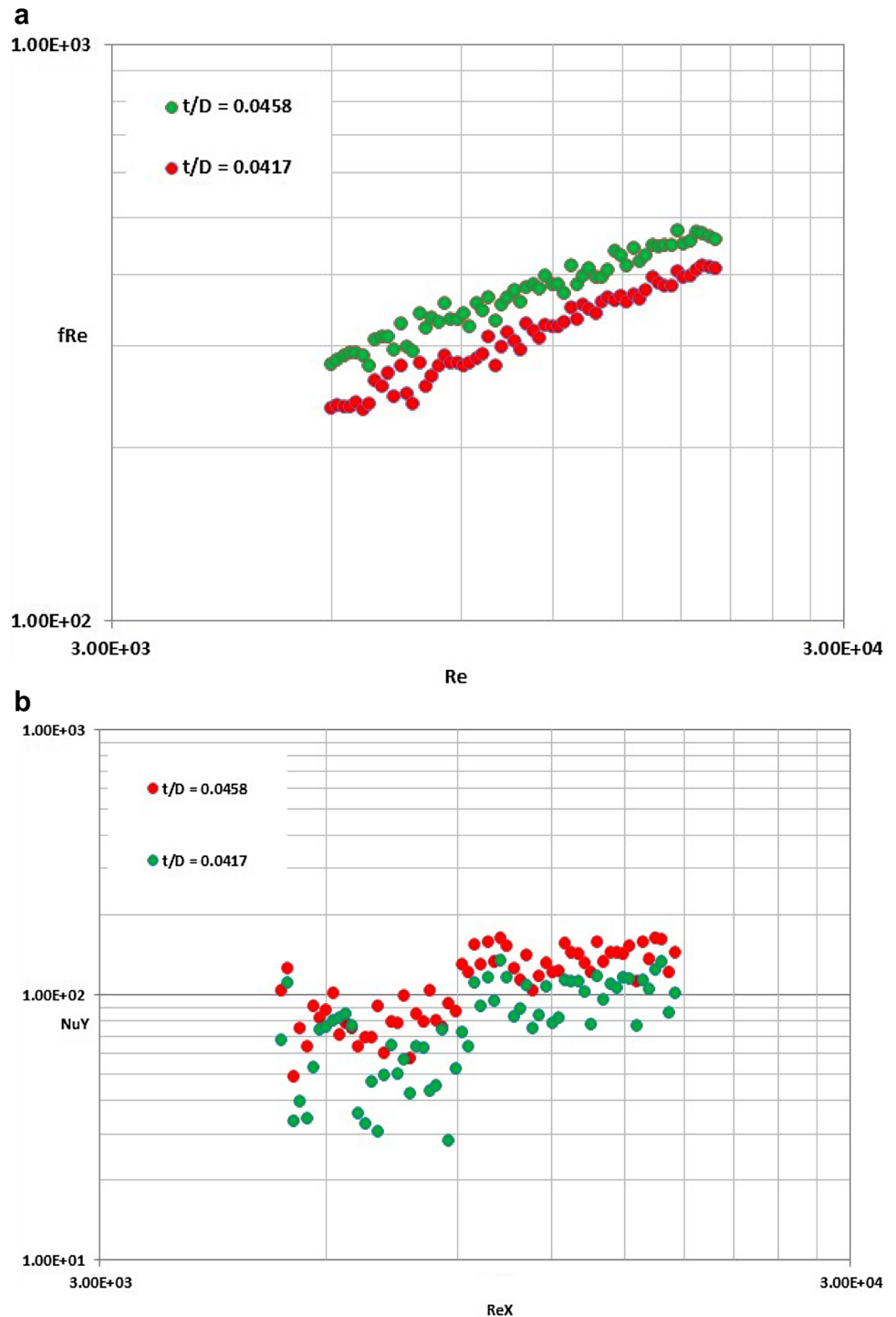
$$Re = \frac{\rho v D_i}{\mu} \tag{7}$$

The friction factor is evaluated by

$$f = \frac{2}{D_i} \frac{\Delta P}{\rho v^2} \tag{8}$$

where  $\Delta P$  is the pressure drop across the test section and  $v$  is the mean air velocity of the duct channel.

**Fig. 5 a** Effect of tape thickness ratio on friction factor, full-length twisted tape: at constant twist ratio  $\gamma = 15.0$  and diameter ratio  $d = 0.83$ , **b** effect of tape thickness ratio on Nu, full-length twisted tape: at constant twist ratio  $\gamma = 15.0$  and diameter ratio  $d = 0.83$



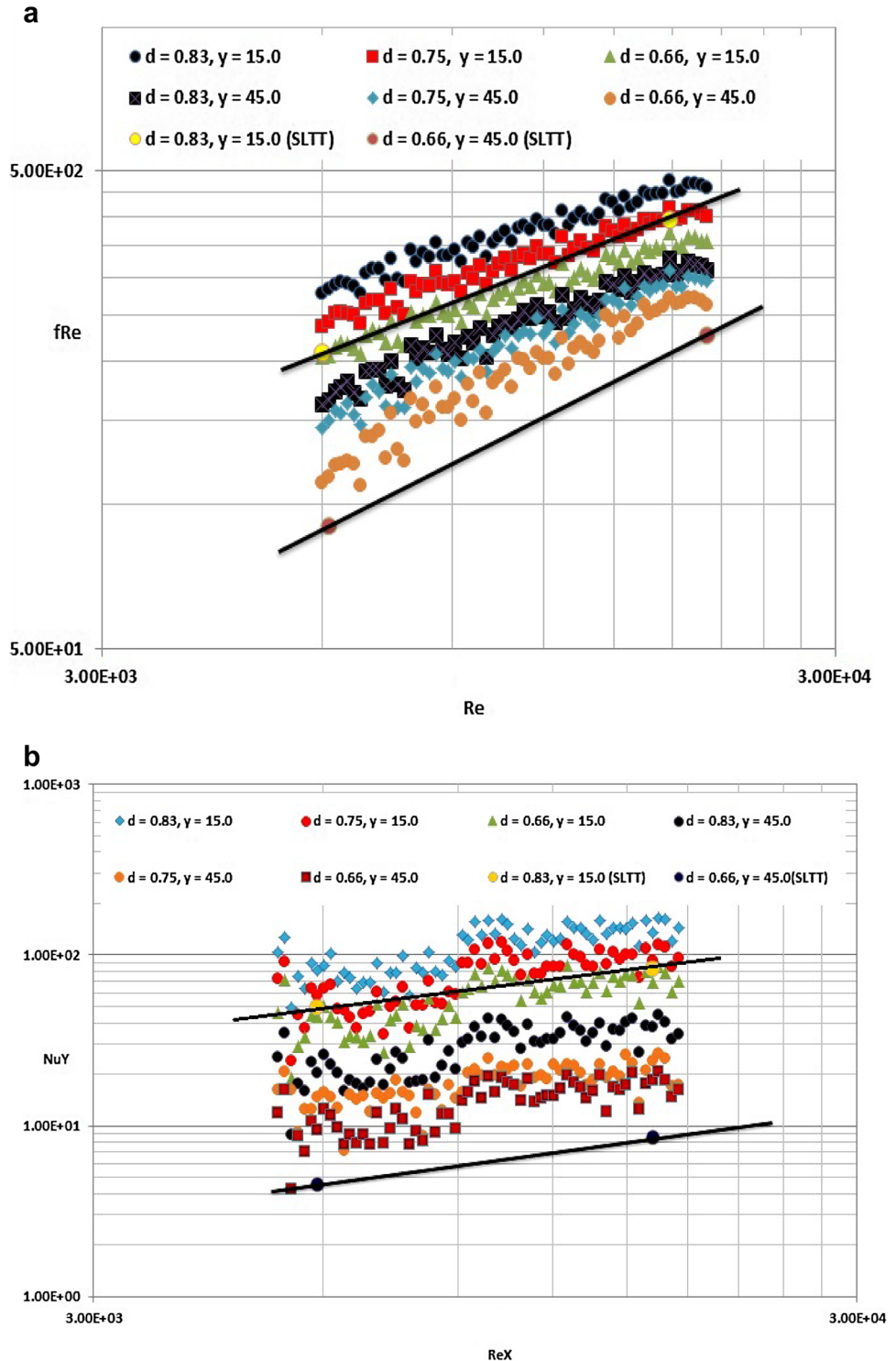
## 4 Results and Discussion

In this division, results of the present experimental investigation are presented and discussed.

Firstly, plain channel without twisted tape is investigated experimentally as shown in Fig. 3. Here, the results

are compared with the empirical correlations by Gnielinski (1985) for the Nusselt number, and friction factor in the turbulent region. A quite good agreement with the present predictions and the present experiments is observed in Fig. 3a, b. Also, the results of the present study are very close to those reported by the same research group

**Fig. 6 a** Effect of diameter ratio and twist ratio on friction factor, full-length twisted tape: at constant twist tape thickness ratio  $\delta = 0.0458$ , **b** effect of diameter ratio and twist ratio on Nu, full-length twisted tape: at constant tape thickness ratio  $\delta = 0.0458$



(Bhattacharyya et al. 2018; Eiamsa-ard and Promvonge 2005; SEiamsa-ard et al. 2009) and are shown in Fig. 3c, d. The considerable deviation of the present study from those reported in the other works may relate to the difference of the geometric parameters of the turbulator channels.

Gnielinski correlation (Ozisik 1985) is as follows:

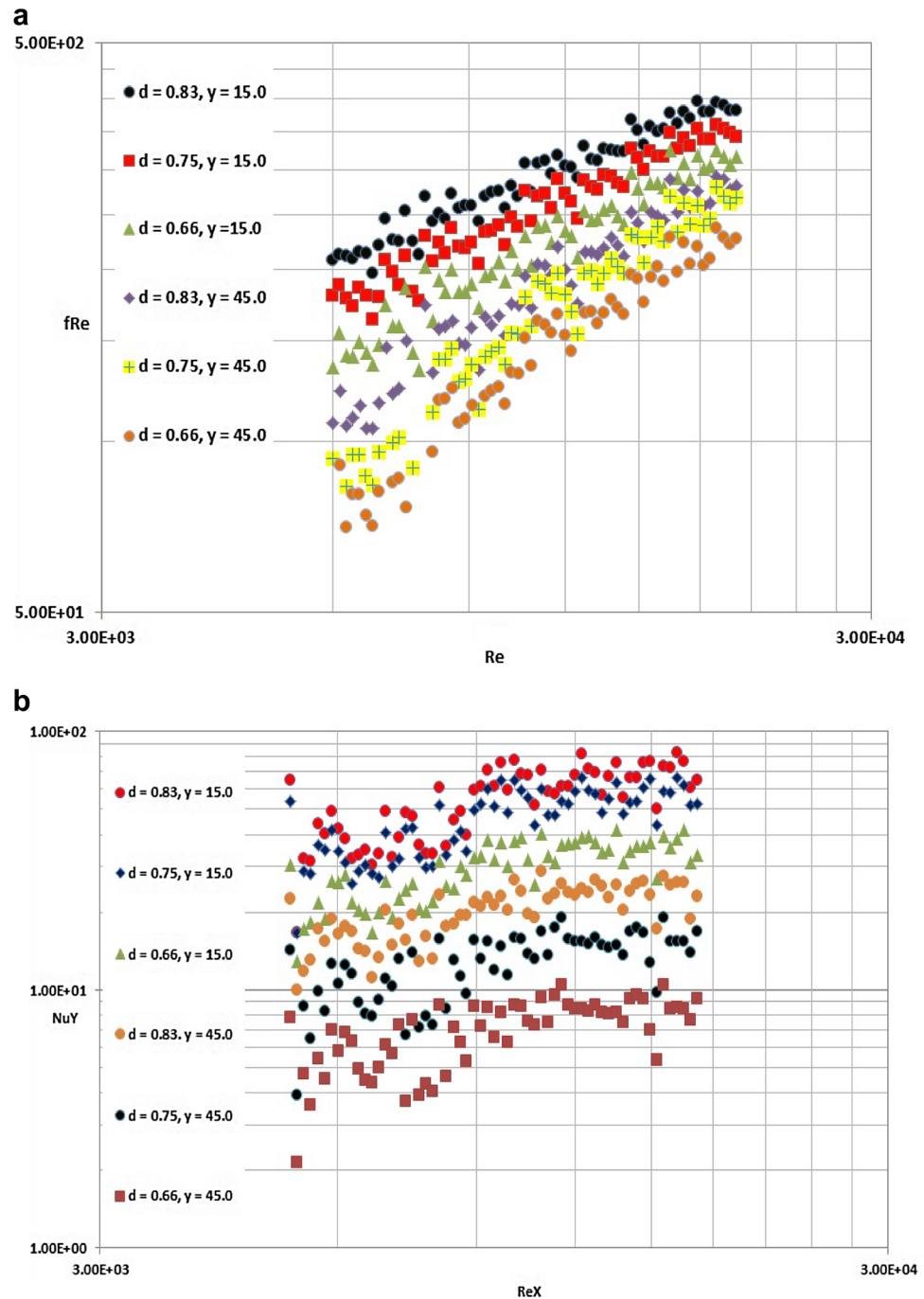
$$Nu = \frac{(f/8)(Re - 1000)Pr}{1 + 12.7(f/8)^{1/2}(Pr^{2/3} - 1)} \tag{9}$$

$$f = (0.79 \ln(Re) - 1.64)^{-2} \tag{10}$$

The friction factor and Nusselt number are solid functions of twist ratios. The effect of twist ratio with  $y = 15.0$



**Fig. 7 a** Effect of diameter ratio and twist ratio on friction factor, short-length twisted tape: at constant twist tape thickness ratio  $\delta = 0.0458$ , **b** effect of diameter ratio and twist ratio on Nu, short-length twisted tape: at constant tape thickness ratio  $\delta = 0.0458$



and 45.0 at constant  $t/D = 0.0417$ ,  $d = 0.75$  and 0.66 of the twisted tape has not been presented separately since the results with  $y = 15.0$  and 45.0 at constant  $t/D = 0.0458$  and  $d = 0.83$  were similar as shown in Fig. 4. Twisted tape of twist ratio  $y = 15.0$  promisingly enhances the heat transfer rate than the tape of twist ratio  $y = 45.0$ ; this is due to the increased turbulence intensity (TI) which helps in disrupting a thermal boundary layer thickness. Furthermore, the interaction among the secondary flows made by the swirl generators also facilitates the disruption of the

viscous sub-layer near channel wall resulting in greater heat transfer enhancement. The flow wavering due to the change of tape twist ratio causes the formation of vortices which further enhance turbulence and thus convective heat transfer rate. The result is expected and it is explained by the fact that, in case of twisted tape of twist ratio  $y = 45.0$ , it cannot provide much of swirl flow and mixing of fluids; hence, there is the disturbance of the boundary layer formation in a dominant manner.

**Table 2** Performance ratios of  $R_1$  and  $R_2$ 

	$(d)_1$		$(d)_2$		$(d)_3$	
	$(y)_1$	$(y)_2$	$(y)_1$	$(y)_2$	$(y)_1$	$(y)_2$
$(t/D)_1 = 0.0458$						
$R_1$	1.23	1.36	1.22	1.35	1.37	1.39
$R_2$	0.61	0.71	0.70	0.81	0.73	0.69
$(t/D)_1 = 0.0417$						
$R_1$	1.36	1.33	1.25	1.33	1.24	1.31
$R_2$	0.63	0.56	0.57	0.73	0.67	0.72
$(t/D)_1 = 0.0458, (t/D)_2 = 0.0417, (d)_1 = 0.83, (d)_2 = 0.75, (d)_3 = 0.66, (y)_1 = 15.0, (y)_2 = 45.0$						

Tape thickness is an important parameter in this study. Tape thickness plays a major role in enhancing heat transfer. There are both pressure drop and heat transfer decrease with the decrease in the value of tape thickness ratio as shown in Fig. 5. Whether the geometry of the channel is circular or non-circular, the effect of twisted tape thickness on friction factor is almost the same; this is correct for all sorts of twisted tapes. The friction factor and Nusselt number increase with the increase in tape thickness ratio.

The experimental results of heat transfer of the channel fitted with SLTT and FLTT under constant heat flux condition are shown in Fig. 6. The FLTT ( $L/D = 90$ ) shows some promising results in terms of heat transfer compared with the SLTT ( $L/D = 54$ ). This is due to continuous swirl flow throughout the test section; also it destroys the thermal boundary layer more than that of SLTT. The stronger swirl flow causes higher TI, better fluid mixing and thus superior heat transfer. So, this can clarify the FLTT prompts swirling flow more than SLTT which is beneficial to stimulating the fluid mixing inside the channel. As a result, FLTT increases the mixing rate of the fluids. Although both the tapes (SLTT and FLTT) provide strong swirl flow at the channel entry. Similarly, it is observed that for the channel with both twisted tapes (SLTT and FLTT) there is a considerable rise in the flow friction than for the channel without twisted tape. The flow friction of SLTT is found to decrease in comparison with FLTT. This is due to the decrease in length ratio ( $L/D$ ) which provides lower swirling strength, which leads to low pressure penalty.

Diameter ratio also plays an important role in enhancing heat transfer inside a channel. For large diameter ratio,  $d = 0.83$  in Fig. 7, an improvement of heat transfer is observed throughout the varied Reynolds numbers range than the other two tested diameter ratios (0.75 and 0.66). However, friction factor increases with the increase in Reynolds number. This is due to the increase in the tape friction in the initial stages.

Performance of the present duct geometry has been evaluated on the basis of performance criteria defined by Bergles et al. (1974). Bergles et al. (1974) have suggested several criteria for the performance evaluation of enhancement devices. The performance of the present geometry has been evaluated on the basis of the following two important criteria:

*Criterion 1* Basic geometry fixed, pumping power fixed—increase heat transfer—performance ratio  $R_1$ .

*Criterion 2* Basic geometry fixed, heat duty fixed—reduce pumping power—performance ratio  $R_2$ .

The subscripts ‘SLTT’ and ‘FLTT’ refer to short-length twisted tape and full-length twisted tape, respectively

$$R_1 = \frac{Nu_{FLTT}}{Nu_{SLTT}} \quad (11)$$

$$R_2 = \frac{(fRe^3Ac)_{FLTT}}{(fRe^3Ac)_{SLTT}} \quad (12)$$

The pumping power reduces up to 27% for full-length twisted tape cases compared to short-length twisted tape at constant heat duty. Similarly, heat duty increases up to 33% as shown in Table 2 at constant pumping power.

## 5 Conclusion

The thermohydraulic characteristics of turbulent flow of air through circular channels with twisted tape turbulators inserts have been investigated experimentally. For the SLTT and FLTT arrangement, three different diameter ratios ( $d$ ), two different twist ratios ( $y$ ) and two different tape thickness ratios ( $\delta$ ) are studied for Reynolds numbers ( $Re$ ) varying from 6000 to 20,000.

Thus, among the considered arrangements, the highest Nusselt number values are obtained for the case  $d = 0.83$ ,  $y = 15$  (applicable for both FLTT and SLTT), compared to the other tested tape and plain channel, over the considered range of  $Re$ . The case  $d = 0.66$ ,  $y = 45$  (applicable for both FLTT and SLTT) gives the minimum Nusselt number values, which are, however, still larger than those of the plain channel. For all  $Re$ , heat transfer is observed to increase with the increasing tape thickness ratio and diameter ratio but decrease with increasing twist ratio. FLTT was found considerably superior than SLTT.

## References

- AI-Fahed S, Chakroun W (1996) Effect of tube tape clearance on heat transfer for fully developed turbulent flow in a horizontal isothermal tube. *Int J Heat Fluid Flow* 17(2):173–178

- Balachandar C, Arunkumar S, Madhumitha R, Venkatesan M (2018) MANFIS–GA heat transfer analysis and optimization of fins with elliptical perforation. *Iran J Sci Technol Trans Mech Eng*. <https://doi.org/10.1007/s40997-018-0179-4>
- Bergles AE, Blumenkrantz AR, Taborek J (1974) Performance evaluation criteria for enhanced heat transfer surfaces. Paper FC 6.3. In: Proceedings of the 5th international heat transfer conference, vol II, Tokyo, pp 239–243
- Bhattacharyya S, Saha SK (2012) Thermohydraulics of laminar flow through a circular tube having integral helical rib roughness and fitted with centre cleared twisted-tape. *Exp Therm Fluid Sci* 42:154–162
- Bhattacharyya S, Saha S, Saha SK (2013) Laminar flow heat transfer enhancement in a circular tube having integral spiral rib roughness and fitted with centre cleared twisted-tape. *Exp Therm Fluid Sci* 44:727–735
- Bhattacharyya S, Chattopadhyay H, Haldar A (2018) Design of twisted tape turbulator at different entrance angle for heat transfer enhancement in a solar heater. *Beni-Suef Univ J Basic Appl Sci* 7(1):118–126
- Eiamsa-ard S, Promvong P (2005) Enhancement of heat transfer in a tube with regularly-spaced helical tape swirl generators. *Sol Energy* 78:483–494
- Eiamsa-ard S, Thianpong C, Eiamsa-ard P, Promvong P (2009) Convective heat transfer in a circular tube with short-length twisted tape insert. *Int Commun Heat Mass Transf* 36:365–371
- Ghajar AJ, Tang CC, Cook WL (2010) Experimental investigation of friction factor in the transition region for water flow in minitubes and microtubes. *Heat Transf Eng* 31(8):646–657
- Manglik RM, Bergles AE (1994) Fully developed laminar heat transfer in circular-segment ducts with uniform wall temperature. *Numer Heat Transf Part A Appl* 26:499–519
- Meyer JP, Abolarin SM (2018) Heat transfer and pressure drop in the transitional flow regime for a smooth circular tube with twisted tape inserts and a square edge inlet. *Int J Heat Mass Transf* 117:11–29
- Meyer JP, Olivier JA (2011) Transitional flow inside enhanced tubes for fully developed and developing flow with different types of inlet disturbances: part I—adiabatic pressure drops. *Int J Heat Mass Transf* 54(7–8):1587–1597
- Mohammadiun H, Amerian V, Mohammadiun M, Rahimi AB (2017) Similarity solution of axisymmetric stagnation-point flow and heat transfer of a nanofluid on a stationary cylinder with constant wall temperature. *Iran J Sci Technol Trans Mech Eng* 41:91–95
- Ozisik MN (1985) *Heat transfer*. McGraw-Hill, New York
- Rahimi M, Soran RA (2017) Numerical analysis of heat transfer and flow field due to slot air jet impingement for the cases of moving plate and moving nozzle. *Iran J Sci Technol Trans Mech Eng* 41:217
- Roy S, Saha SK (2015) Thermal and friction characteristics of laminar flow through a circular duct having helical screw-tape with oblique teeth inserts and wire coil inserts. *Exp Therm Fluid Sci* 68:733–743
- Sabet GS, Pavithran S, Iran Kulkarni RR (2017) comparison of heat transfer enhancement in a diffuser by inserting wing vortex generators and protrusions. *Iran J Sci Technol Trans Mech Eng*. <https://doi.org/10.1007/s40997-017-0084-2>
- Saha SK (2010) Thermohydraulics of turbulent flow through rectangular and square ducts with axial corrugation roughness and twisted tapes with and without oblique teeth. *Exp Therm Fluid Sci* 34(6):744–752
- Saha SK (2011) Thermohydraulics of turbulent flow through square and rectangular ducts with transverse ribs and twisted tapes with and without oblique teeth. *J Enhanc Heat Transf* 18(4):281–293
- Saha SK, Bhattacharyya S, Pal PK (2012) Thermo-hydraulics of laminar flow of viscous oil through a circular tube having integral spiral rib roughness and fitted with centre-cleared twisted tape. *Exp Therm Fluid Sci* 41:121–129
- Sheikholeslami M (2018a) Numerical investigation for CuO–H<sub>2</sub>O nanofluid flow in a porous channel with magnetic field using mesoscopic method. *J Mol Liq* 249:739–746
- Sheikholeslami M (2018b) Numerical investigation of nanofluid free convection under the influence of electric field in a porous enclosure. *J Mol Liq* 249:1212–1221
- Sheikholeslami M, Ganji DD (2016a) Heat transfer improvement in a double pipe heat exchanger by means of perforated turbulators. *Energy Convers Manag* 127:112–123
- Sheikholeslami M, Ganji DD (2016b) Heat transfer enhancement in an air to water heat exchanger with discontinuous helical turbulators; experimental and numerical studies. *Energy* 116:341–352
- Sheikholeslami M, Rokni HB (2018) Numerical simulation for impact of Coulomb force on nanofluid heat transfer in a porous enclosure in presence of thermal radiation. *Int J Heat Mass Transf* 118:823–831
- Sheikholeslami M, Seyednezhad M (2018) Simulation of nanofluid flow and natural convection in a porous media under the influence of electric field using CVFEM. *Int J Heat Mass Transf* 120:772–781
- Sheikholeslami M, Shehzad SA (2018) Simulation of water based nanofluid convective flow inside a porous enclosure via non-equilibrium model. *Int J Heat Mass Transf* 120:1200–1212
- Sheikholeslami M, Darzi M, Sadoughi MK (2018) Heat transfer improvement and pressure drop during condensation of refrigerant-based nanofluid; an experimental procedure. *Int J Heat Mass Transf* 122:643–650
- Sivashanmugam P, Suresh S (2006) Experimental studies on heat transfer and friction factor characteristics of laminar flow through a circular tube fitted with helical screw-tape inserts. *Appl Therm Eng* 26:1990–1997
- Sivashanmugam P, Suresh S (2007a) Experimental studies on heat transfer and friction factor characteristics of laminar flow through a circular tube fitted with regularly spaced helical screw-tape inserts. *Exp Therm Fluid Sci* 31:301–308
- Sivashanmugam P, Suresh S (2007b) Experimental studies on heat transfer and friction factor characteristics of turbulent flow through a circular tube fitted with regularly spaced helical screw-tape inserts. *Appl Therm Eng* 27:1311–1319
- Sivashanmugam P, Suresh S (2007c) Experimental studies on heat transfer and friction factor characteristics of turbulent flow through a circular tube fitted with helical screw-tape inserts. *Chem Eng Process* 46:1292–1298
- Suresh KP, Mahanta P, Dewan A (2004) Study of heat transfer and pressure drop in a large hydraulic diameter annulus. In: 17th national heat and mass transfer conference and 6th ISHMT/ASME, heat and mass transfer conference. Indira Gandhi Centre for Atomic Research, Kalpakkam, pp 62–66
- Tiwari M, Saha SK (2015) Thermohydraulics of laminar flow through a circular tube with transverse ribs and twisted tapes. *ASME J Therm Sci Eng Appl* 7(4):041009. <https://doi.org/10.1115/1.4030792>